Phys. Status Solidi B **250**, No. 9, 1816–1824 (2013) / **DOI** 10.1002/pssb.201248378

physica status solidi b
www.pss-b.com
basic solid state physics

Microscopic approach to the magnetoelectric effect in $R\mathrm{Mn_2O_5}$

Safa Golrokh Bahoosh,[1] Julia M. Wesselinowa,[2] and Steffen Trimper[3]

[1] Max Planck Institute of Microstructure Physics, Weinberg 2, 06120 Halle, Germany
[2] Department of Physics, University of Sofia, Blvd. J. Bouchier 5, 1164 Sofia, Bulgaria
[3] Institute of Physics, Martin-Luther-University, Von-Seckendorff-Platz 1, 06120 Halle, Germany

Received 15 August 2012, revised 2 April 2013, accepted 16 April 2013
Published online 23 May 2013

Keywords magnetoelectric coupling, magnetization, polarization

Corresponding author: e-mail steffen.trimper@physik.uni-halle.de, Phone:+49 345 55 25432, Fax:+49 345 55 25446

The multiferroic behavior of rare-earth manganites is studied within a microscopic model including a symmetry-allowed magnetoelectric coupling between polarization and magnetization. The magnetic subsystem is described by a frustrated Heisenberg spin model, whereas the ferroelectric subsystem is characterized by an Ising model in a transverse field. Using Green's function method we find analytically the temperature and wave vector dependent elementary excitation of the magnetoelectric system, the polarization and the magnetization for different magnetoelectric coupling strengths. The system undergoes a magnetic transition at T_N and a further reduction of the temperature leads to a ferroelectric transition at $T_C < T_N$ depending on the coupling strength. That coupling is also manifested as a kink in the magnetization and the elementary excitation at T_C. Due to the magnetoelectric coupling the excitation energy exhibits a gap at zero wave vector which increases with increasing coupling. We show that the macroscopic magnetization can be slightly enhanced by an external electric field nearby T_C. An external magnetic field leads to an increase of the polarization.

1 Introduction There is currently a great effort in understanding the microscopic nature of the coupling between ferroelectric and magnetic ordering in several transition metal oxides such as $R\mathrm{Mn_2O_5}$ where R represents rare-earth elements [1–4]. As argued [5, 6] the ferroelectricity is driven by the magnetic ordering, i.e the material possess a strong magnetoelectric coupling (MEC). The kind of MEC is responsible for the sensitivity of the system to applied magnetic fields and may lead to new classes of functional materials. One of the key compounds that has triggered such research activity is $\mathrm{TbMn_2O_5}$, in which a continuous actuation of electric polarization P is realized at low magnetic field $H < 2$T. Numerous studies of this material and related ones like $R\mathrm{Mn_2O_5}$ have shown that spatially modulating, noncollinear magnetic order due to spin frustration is the reason for inducing a ferroelectric order in those materials. More specifically, the main mechanism for the appearance of a nontrivial polarization P in $R\mathrm{Mn_2O_5}$ (R = Tb, Y, Dy, and Bi) has been attributed to exchange-striction among frustrated Mn spin networks [7], while a contribution to the polarization due to a spiral spin order is relevant in $R\mathrm{Mn_2O_5}$ (R = Ho, Er, and Tm) [8]. The dominant mechanism for developing a nonzero polarization in $R\mathrm{Mn_2O_5}$ seems to be associated with the order of the spins of Mn [9]. This fact is related to the complexity of the $R\mathrm{Mn_2O_5}$ crystal structure, where $\mathrm{Mn^{4+}O_6}$ octahedra and $\mathrm{Mn^{3+}O_5}$ pyramids are linked through edge- and corner-sharing networks. As a result one can discriminate five independent nearest-neighbor magnetic interactions [10]. There is a limited number of works discussing the possible effects of rare-earth ions on the temperature and magnetic field dependence of the polarization P on $R\mathrm{Mn_2O_5}$ [11–14]. So the role of the rare-earth ions in $R\mathrm{Mn_2O_5}$ is far from being completely understood, in particular, the manipulation of the polarization by an external magnetic field is of interest. Such an effect is uniquely realized in $\mathrm{TbMn_2O_5}$. Several studies of the magnetic properties as function of the temperature have indicated that $R\mathrm{Mn_2O_5}$ compounds are ferroelectric in their magnetically ordered state [15–18]. A kink in the magnetization [15–17] or in the magnetic susceptibility [18] at the ferroelectric phase transition temperature is observed, which give a strong evidence of a MEC in these substances.

The known microscopic mechanisms of magnetically induced ferroelectricity include lattice distortion (exchange-striction) and redistribution of electron density in response

to the spin ordering. Such processes occur locally in all magnetic materials. However, only when a spin ordering breaks the inversion symmetry these local electric dipoles sum up to a macroscopic electric polarization. Good candidates of spin orders breaking inversion symmetry are frustrated magnets, where competing interactions and the geometry of spin lattice favors unconventional magnetic states. In most of the recently discovered multiferroic materials such competing interactions force the spins to generate a cycloidal spiral. This non-collinear spin order breaks the inversion symmetry and activates for instance an antisymmetric Dzyaloshinskii–Moriya interaction proportional to the cross-product of spins, $\boldsymbol{S}_1 \times \boldsymbol{S}_2$ [19]. In case inversion symmetry is broken by a collinear magnetic ordering the dominant spin interaction that can shift ions and polarize electronic clouds is the Heisenberg exchange coupling proportional to the scalar product of spins $\boldsymbol{S}_1 \cdot \boldsymbol{S}_2$. This mechanism is used to explain the multiferroic properties of $R\mathrm{Mn_2O_5}$, where R denotes a rare earth ions, Y or Bi, and orthorhombic manganites offer the E-type antiferromagnetic ordering [20]. In that paper [20] a microscopic model is discussed based on the assumption that the mechanism of magnetically induced ferroelectricity and electromagnon absorption relies entirely on the isotropic Heisenberg exchange and additional magnetostrictive coupling of spins to a polar lattice mode. So relativistic effects are not involved. Another approach is due to [21] where an effective model was developed to explain the mechanism of magnetoelectric coupling in multiferroic $R\mathrm{Mn_2O_5}$ and the related phase diagram. The origin of the magnetoelectric effect in $R\mathrm{Mn_2O_5}$ is a coupling between two Ising-type orders, namely the ferroelectric order along the b-axis, and the coupled magnetic order between two frustrated antiferromagnetic chains. Based on the exchange-striction mechanism, a model is proposed in Ref. [22] with the intent to capture the interplay between spin and dipolar moments in the presence of a magnetic field in $\mathrm{BiMn_2O_5}$. The magnetic properties of $R\mathrm{Mn_2O_5}$ multiferroics were reviewed in Ref. [23] using unpolarized and polarized neutron diffraction experiments. The nature of ferroelectricity is based on calculations of the ferroelectric polarization predicted by different microscopic coupling mechanisms (exchange-striction and cycloidal spin-orbit models). A minimal model including a small set of parameters is also presented in order to understand the propagation of the magnetic structure along the c-direction. To that aim an effective spin Hamiltonian for $\mathrm{YMn_2O_5}$ were constructed [24] and studied by density-functional theory. Using the related first-principles-derived spin Hamiltonian the authors have calculated the magnon dispersion relation for this compound and compared it with the experimentally measured spectra probed using inelastic neutron scattering. The magnetostructural transitions and the magnetoelectric effects reported for $\mathrm{TbMn_2O_5}$ are described in Ref. [25] theoretically. The ground state as well as structural, electronic, and magnetic properties of multiferroic $\mathrm{TbMn_2O_5}$ via first-principles calculations were found by Wang et al. [6]. Due to this work the ferroelectricity in $\mathrm{TbMn_2O_5}$ is driven by the non-centrosymmetric magnetic ordering, without invoking the spin-orbit coupling and non-collinear spins.

In spite of a broad variety of effects occurring in multiferroic material a detailed analysis of underlying quantum models is still lacking. Therefore the goal of the present paper is to propose and to analyze a microscopic model for rare-earth manganites. The model comprises three items, the frustrated magnetic subsystem characterized by competing magnetic interactions, the ferroelectric subsystem characterized by an Ising model in a transverse field [26–28] and the magnetoelectric coupling. That coupling between both subsystems is allowed by symmetry and includes a quadratic magnetic order parameter and a linear polar order parameter. The analysis is performed in such a manner that the MEC triggers the transition to the ferroelectric phase. An appropriate tool to investigate such a quantum model analytically is the method of thermodynamic Green's function. The poles of the Green's function yields the spectrum of the elementary excitations, which, on the other hand determine the macroscopic quantities like polarization and magnetization as functions of temperature and the magnetoelectric coupling constant. The excitation spectrum offers a gap due to the MEC. The model can be extended by inclusion the coupling of external electric and magnetic fields. We demonstrate that the magnetization is affected by an electric field and the polarization by the corresponding magnetic field

2 The model So far, two distinct scenarios have been proposed for the microscopic mechanism of magnetically induced ferroelectricity. Many of the recently discovered multiferroic materials, such as $\mathrm{TbMnO_3}$ and $\mathrm{MnWO_4}$, show cycloidal spin order attributed to frustration due to competing interactions [2, 29]. In these systems, non-collinear magnetic orders break inversion symmetry and give rise to polarization via the antisymmetric Dzyaloshinskii–Moriya interaction. The resulting polarization is induced by a pair of spins and is given by $P \propto \boldsymbol{S}_1 \times \boldsymbol{S}_2$. On the other hand, a configuration of collinear spins breaking the inversion symmetry can induce polarization via a mechanism based on the isotropic Heisenberg exchange and a magnetostrictive coupling of spins to a polar lattice mode. In this case the polarization is related to $P \propto \boldsymbol{S}_1 \cdot \boldsymbol{S}_2$. The last mechanism was proposed to explain the properties of orthorhombic manganites $R\mathrm{Mn_2O_5}$ [30]. Here we follow the second way where different to other approaches the ferroelectric subsystem is described by an Ising model in a transverse field. This model reflects the physical situation in a more adequate manner. The broad spectrum of the Ising model in a transverse field in studying ferroelectric behavior has been demonstrated recently [28, 27]. The model can be successfully applied for a large class of ferroelectric materials.

2.1 Hamiltonian The Hamiltonian of the model can be written as:

$$H = H_m + H_f + H_{mf}. \tag{1}$$

The Hamiltonian of the magnetic subsystem H_m is given by the Heisenberg model including nearest neighbor ferromagnetic coupling $J > 0$ and next nearest antiferromagnetic coupling $\tilde{J} > 0$:

$$H_m = -\frac{1}{2}\sum_{ij} J_{ij}\boldsymbol{S}_i \cdot \boldsymbol{S}_j + \frac{1}{2}\sum_{\langle ij\rangle} \tilde{J}_{ij}\boldsymbol{S}_i \cdot \boldsymbol{S}_j. \tag{2}$$

The sum over all next nearest neighbors is indicated by $\langle ij\rangle$. Due to the competition between ferromagnetic and antiferromagnetic order the magnetic subsystem is able to develop frustration if $\tilde{J} > J/4$ [31]. Otherwise we are aware that the modeling of the magnetic subsystem by the Hamiltonian in Eq. (2) is an approximation. As discussed in Ref. [10, 32] the magnetic behavior is characterized by five different coupling parameters within the spin Hamiltonian. Due to [33] adjacent Mn^{3+} and Mn^{4+} ions are coupled antiferromagnetically. As pointed out this fact leads to magnetic frustration. Because an analytical modeling of an Heisenberg spin model with five independent exchange couplings is too comprehensive we have simplified the model by including two couplings which leads however to frustration.

The ferroelectric behavior is modeled by the Ising model in a transverse field (TIM), the relevance of which is discussed in Refs. [26, 27], for a recent review compare [28]. The Hamiltonian reads

$$H_f = -\frac{1}{2}\sum_{ij} J'_{ij}B_i^z B_j^z - 2\Omega\sum_i B_i^x. \tag{3}$$

Here the pseudo-spin operator B_i^z characterizes the two position of the ferroelectric unit at the lattice point i. These two positions are separated by a barrier. The interaction between adjacent lattice sites is denoted by J'_{ij}. The dynamics of the model with strength Ω is determined by the operator B^x. This term is responsible for overcoming the barrier between the two positions. It describes the flipping process between both wells. Therefore Ω is sometimes called tunneling frequency. Let us stress that the operators $\boldsymbol{B}_i$ are pseudo-spin operators which fulfill the commutation relation of conventional spin operators but have nothing to do with real spins of the ferroelectric units.

The last term in Eq. (1) describes the coupling between the magnetic and the ferroelectric subsystems. As shown by [20, 21] the material allows a coupling of the general form

$$H_{mf} = \sum_{ijl} K_{ijl}B_i^z \boldsymbol{S}_j \cdot \boldsymbol{S}_l. \tag{4}$$

For the subsequent calculations we need only the coupling at zero wave vector. So, the MEC should be written with a (pseudo)-scalar coupling K instead of K_{ijl}. The parameter K is a measure for the coupling strength between the magnetic and the electric order parameters.

To study the magnetic subsystem it is appropriate to introduce spin-ladder operators $S^{\pm} = S^x \pm iS^y$ leading to

$$H_m = -\frac{1}{2}\sum_{i,j} J_{ij}(S_i^+ S_j^- + S_i^z S_j^z) + \frac{1}{2}\sum_{\langle i,j\rangle} \tilde{J}_{il}(S_i^+ S_j^- + S_i^z S_j^z). \tag{5}$$

Here i, j means summation over nearest neighbors whereas $\langle i, j\rangle$ denotes next nearest neighbors. Because the ferroelectric part H_f in Eq. (3) suggests that both mean values $\langle B^z\rangle$ and $\langle B^x\rangle$ are nonzero in the ordered phase, it seems to be appropriate to introduce a rotated frame according to

$$\begin{aligned} B_i^x &= \left(\frac{1}{2} - \rho_i\right)\sin\nu + \frac{1}{2}\left(b_i + b_i^\dagger\right)\cos\nu, \\ B_i^y &= \frac{i}{2}(b_i^\dagger - b_i), \\ B_i^z &= \left(\frac{1}{2} - \rho_i\right)\cos\nu - \frac{1}{2}\left(b_i + b_i^\dagger\right)\sin\nu. \end{aligned} \tag{6}$$

The angle is determined in such a manner that $\langle B^x\rangle = 0$ after rotation. Moreover the determination of the angle guarantees that the ferroelectricity is induced by the magnetic behavior and is triggered by the MEC. Insofar the model describes improper ferroelectricity. Notice that in Eq. (6) b and $b^\dagger$ are Pauli-operators which fulfill the commutator relation $[b_i, b_j^\dagger] = (1 - 2\rho_i)\delta_{ij}$ with $\rho_i = b_i^\dagger b_i$. Both Hamiltonian H_f and H_{mf} in terms of Pauli-operators can be found in the appendix. The model system will be analyzed in terms of Green's function introduced in the following subsection.

2.2 Green's functions and results As already mentioned the method of thermodynamic Green's function [34] allows to find the dispersion relation of the elementary excitation of the underlying quantum model, and moreover the temperature dependent macroscopic quantities as magnetization and polarization. In particular, the poles of the Green's function will be identified with the spectrum of the excitations. To be specific let us define for the magnetic part the Green's function by [34]:

$$\begin{aligned} G_{lm}^{(m)}(t - t') &\equiv \langle\langle S_l^+(t); S_m^-(t')\rangle\rangle \\ &= -i\Theta(t - t')\langle[S_l^+(t)\,, S_m^-(t',]\rangle. \end{aligned} \tag{7}$$

Using the commutation relation and making a simple RPA decoupling [31, 34] it results after Fourier transformation

$$G^{(m)}(\boldsymbol{q}, E) = \frac{2\langle S^z\rangle}{E - E_M(\boldsymbol{q})} \quad \text{with}$$
$$E_M(\boldsymbol{q}) = \langle S^z\rangle\left(J_0 - J_q - \tilde{J}_0 + \tilde{J}_q - 2K_0\langle\sigma_P\rangle\cos\nu\right). \tag{8}$$

The excitation energy of the magnetic spin-waves $E_M(\boldsymbol{q})$ depends on the competing ferromagnetic J and antiferromagnetic couplings $\tilde{J}$, introduced in Eq. (2). Due to MEC the spectrum includes both the magnetization $M = \langle S^z\rangle = \langle\sigma_M\rangle$ as well as the polarization $P = \langle\sigma_P\rangle = \frac{1}{2} - \langle\rho\rangle$. Since the spin of $TbMn_2O_5$ is assumed to be $S = 2$ the calculations of the magnetic system are performed for arbitrary spin. Following [35] we find the magnetization $M \equiv \langle\sigma_M\rangle$:

$$\langle\sigma_M\rangle = \frac{1}{N}\sum_q \left(\left(S+\frac{1}{2}\right)\coth\left[\left(S+\frac{1}{2}\right)\beta E_M(\boldsymbol{q})\right] - 1/2\coth\frac{\beta E_M(\boldsymbol{q})}{2}\right). \quad (9)$$

The analysis of the ferroelectric subsystem is more complex. One needs a matrix Green's function defined by

$$\begin{pmatrix} \langle\langle b_l; b_m^\dagger\rangle\rangle & \langle\langle b_l; b_m\rangle\rangle \\ \langle\langle b_l^\dagger; b_m^\dagger\rangle\rangle & \langle\langle b_l^\dagger; b_m\rangle\rangle \end{pmatrix} \equiv \begin{pmatrix} G_{lm}^{(f)11} & G_{lm}^{(f)12} \\ G_{lm}^{(f)21} & G_{lm}^{(f)22} \end{pmatrix}. \quad (10)$$

The related equations of motion for the Green's function matrix and the results are given in the appendix. In our case we find $\varepsilon_q^{11} = -\varepsilon_q^{22}$ and $\varepsilon_q^{12} = -\varepsilon_q^{21}$. Here we present the result for $G^{(f)11}(\boldsymbol{q}, E)$ in the following form

$$G_q^{(f)11} = \langle\sigma_P\rangle\left(\frac{\epsilon_q}{E-E_F} - \frac{\epsilon'_q}{E+E_F}\right),$$
$$E_F(\boldsymbol{q}) = \sqrt{(\varepsilon_q^{11})^2 - (\varepsilon_q^{12})^2}. \quad (11)$$

The coefficients ϵ_q, ϵ'_q as well as ε_q^{11} and ε_q^{11} can be found in the appendix. The polarization $P = \langle\sigma_P\rangle$ follows as

$$\frac{1}{\langle\sigma_P\rangle} = \frac{2}{N}\sum_q \frac{\varepsilon_q^{11}}{E_F(\boldsymbol{q})}\coth\frac{\beta E_F(\boldsymbol{q})}{2}. \quad (12)$$

As one can observe the excitation energy of the ferroelectric part depends on the rotation angle ν which has to be determined. To that aim we use

$$i\frac{\partial}{\partial t}\langle b_q\rangle = \langle[b_q, H]\rangle = 0.$$

From here we get an equation of the type $A\langle b_q\rangle + B\langle b_q^\dagger\rangle + C = 0$, where A, B, and C are well defined coefficients. Due to $\langle b\rangle = 0$ it results

$$C = (-2\Omega\cos\nu + \tfrac{1}{2}J'_0\sin\nu\cos\nu\langle\sigma_P\rangle)\langle\sigma_P\rangle - \tfrac{1}{2}K_0\sin\nu\langle\sigma_P\rangle\langle\sigma_M\rangle^2. \quad (13)$$

As a nontrivial result we find the equation for the angle ν

$$\tan\nu = \frac{4\Omega}{J'_0\langle\sigma_P\rangle\cos\nu - K_0\langle\sigma_M\rangle^2}. \quad (14)$$

This equation reflects the improper nature of the ferroelectricity. It is magnetically induced and the occurrence of the polarization is strongly related to magnetoelectric coupling K_0. The further analysis is done using the couplings

$$J_q = zJ\cos\left(\frac{1}{2}q_x a\right)\cos\left(\frac{1}{2}q_y a\right)\cos\left(\frac{1}{2}q_z a\right),$$
$$J'_q = zJ'\cos\left(\frac{1}{2}q_x a\right)\cos\left(\frac{1}{2}q_y a\right)\cos\left(\frac{1}{2}q_z a\right),$$
$$\tilde{J}_q = \frac{z'}{3}\tilde{J}(\cos(q_x a) + \cos(q_y a) + \cos(q_z a)), \quad (15)$$

where $z = 8$ is the number of nearest neighbors and $z' = 6$ is the number of next nearest neighbors. Furthermore we have $J_0 = zJ$.

3 Discussion In this section we present the numerical results based on our theoretical calculations where the following model parameters are used for the ferroelectric and the magnetic subsystem: $T_C = 37$ K, $T_N = 44$ K, $J'_0 = 75\ K$, $\Omega = 0.2\ K$, $J_0 = 54\ K$, $\tilde{J} = 18.5\ K$, $K_0 = -7\ K$, pseudospin $S = 1/2$. The spin is $S = 2$. The data are appropriate for $TbMn_2O_5$. The analysis is focused on the magnetization obtained by in Eq. (9), the polarization, Eq. (12), and the spin-wave frequency according to Eq. (8). The temperature dependence of the magnetization M is shown in Fig. 1. Notice that the calculation of the magnetization is based on the spin-wave energy of the magnetic subsystem E_M which is given in Eq. (8). The temperature dependent spin-wave energy E_M at zero wave vector is shown in Fig. 2. In both figures the MEC between the two order parameters is manifested as a kink at the ferroelectric phase transition temperature T_C. This discontinuity in M and E_M characterizes the mutual influence between ferroelectric and magnetic ordering. A simple physical picture behind this effect could be related to an energy transfer

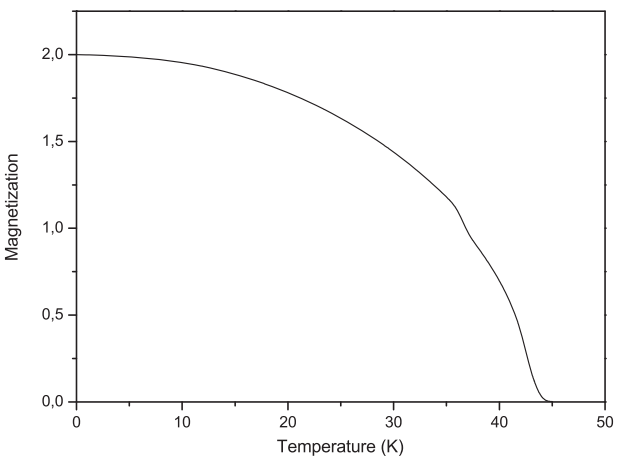

Figure 1 Temperature dependence of the magnetization M with with $J'_0 = 75\ K$ and $K_0 = -7\ K$.

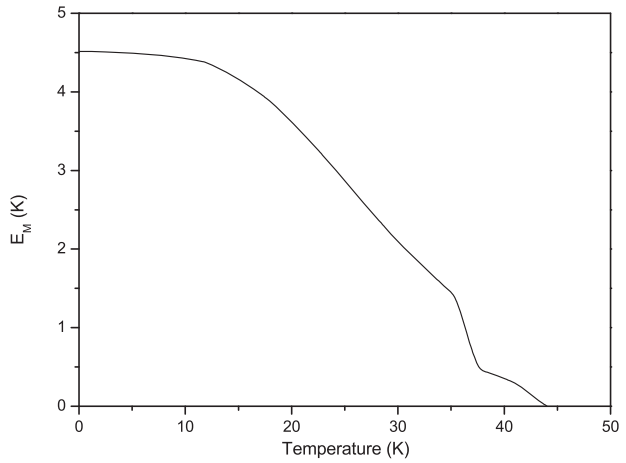

Figure 2 Temperature dependence of the spin-wave energy E_M for zero wave vector with $J_0' = 75\ K$ and $K_0 = -7\ K$.

from the magnetic phase to the polar phase. This energy is necessary to establish the new ferroelectric phase. Because of $T_C < T_N$, the electric subsystem is not able to influence the magnetic one above T_C. The two phases coexist only below T_C. Such a cusp-like anomaly at the ferroelectric critical temperature is obtained experimentally for example in the magnetic susceptibility [18] in $TbMn_2O_5$ and in the magnetization [15–17] of RMn_2O_5 and orthorhombic $RMnO_3$. The kink is an strong indication for the magnetoelectric effect. A similar change, a kink in the temperature dependence of the magnetization at the ferroelectric Curie temperature T_C is reported by Zheng et al. [36] in nano-structured $BaTiO_3$–$CoFe_2O_4$ ferroelectromagnet. The measured specific heat shows kinks at the critical temperatures T_C and T_N in $DyMn_2O_5$ [4]. As shown in Fig. 2 the magnetic excitation offers a novel softening behavior around T_N.

The polarization P decreases with increasing temperature and vanishes at the critical temperature T_C which is depicted in Fig. 3. The polarization offers a phase transition

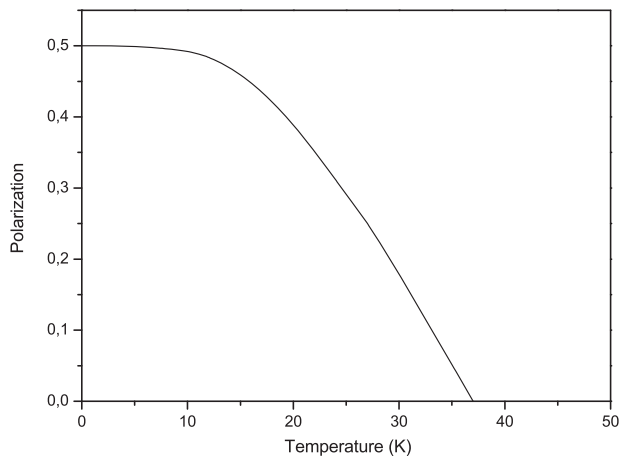

Figure 3 Dependence of the polarization P on the temperature for $J_0' = 75\ K$ and $K_0 = -7\ K$.

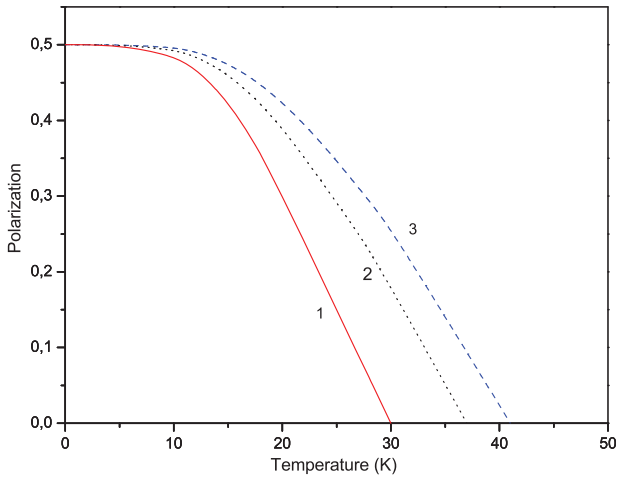

Figure 4 Dependence of the polarization P for different magnetoelectric couplings $K_0 = -3\ K$ (1); $K_0 = -7\ K$ (2); $K_0 = -10\ K$ (3); $J_0' = 75\ K$ and $K_0 = -7\ K$.

at T_C where above T_C the system is disordered and reveals no ferroelectric order. Notice that the spontaneous polarization P exists below T_C where the system is likewise magnetically ordered. Such a behavior is characteristic for multiferroics. The polarization is magnetically induced. In a recent paper [37] the authors have identified three independent contributions to the polarization related to Mn^{3+} and Mn^{4+} as well as to the antiferromagnetic Tb^{3+} order. We argue that this subtle effect could be included in our approach, too. However to that aim, the magnetic part of our model, see Eq. (2), should be extended by including more than two exchange coupling terms following the line given in Ref. [10]. Such an extension of the model is in principle possible but seems to be out of the scope of an analytical approach. A further complication is originated by the different values of the spins which contributes differently to the magnetization accordinng to Eq. (9). Otherwise our model demonstrates clearly the effect and the relevance of the magnetoelectric coupling on the polarization P. As indicated in Fig. 4 the polarization depends strongly on the MEC K_0 introduced in Eq. (4). With increasing coupling K_0 the polarization P is enhanced and the phase transition temperature T_C grows, too. Consequently the discontinuity in the magnetization M and energy E_M at T_C is shifted towards T_N. Moreover the discontinuity in M and E_M becomes more pronounced with enlarged MEC, compare Fig. 5 and Fig. 6. This result seems to us a strong indication for the relevance of the MEC. As mentioned above the discontinuity in M and E_M is related to an energy transfer, which obviously increases the stronger the MEC is. The magnetic phase transition temperature T_N remains essentially unaffected by K_0. The increase of the ferroelectric transition temperature T_C with stronger MEC strength offers mathematically the possibility that $T_C \geq T_N$. Therefore the improper nature of the polar phase is only guaranteed when the coupling parameter K_0 is limited to such values that T_C remains smaller than T_N. The growing T_C is also discussed below where we show that

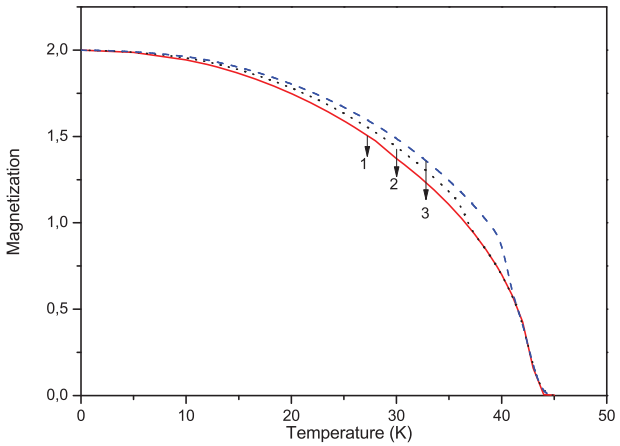

Figure 5 Temperature dependence of the magnetization M for different magnetoelectric couplings: $K_0 = -3\,K$ (1); $-7\,K$ (2); $-10\,K$ (3).

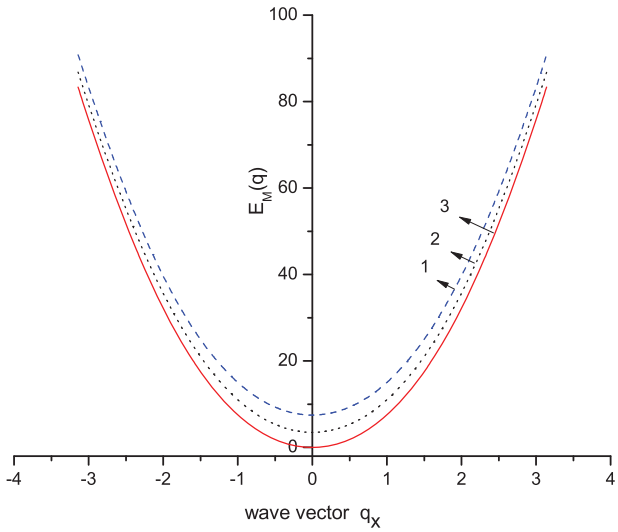

Figure 7 Wave vector dependence of the spin-wave energy E_M for different magnetoelectric coupling constant $K_0 = 0\,K$ (3); $-7\,K$ (2); $-10\,K$ (1).

T_C is enlarged by an increasing external electric field. The magnetic excitation energy $E_M(\boldsymbol{q})$ is also influenced by the MEC K_0. The result for a fixed temperature is shown in Fig. 7.

In the same manner the spin-wave dispersion at zero wave vector is varied for different MEC which is shown in Fig. 6. The dispersion relation $E_M(\boldsymbol{q})$ increases with the wave vector q, see Fig. 7. If the MEC is absent the energy is typically zero at $q = 0$ (curve 3). Due to the non-vanishing MEC the system develops an energy gap at zero wave vector which increases with increasing of the magnetoelectric coupling K_0, see curve 1 and 2 in Fig. 7. The MEC breaks the continuous symmetry of the magnetic subsystem and the related Goldstone mode becomes massive, i.e., the dispersion relation reveals a gap at zero wave vector.

One of the advantage of multiferroic material is the possibility to control the polarization by an external magnetic field h and the magnetization by an external electric field E. Therefore the total Hamiltonian Eq. (1) has to be supplemented by such external field terms. The coupling of both external fields is a linear ones to the spins and to the pseudo-spins, respectively. The strong MEC can be seen by studying the influence of an applied electric field on the magnetic properties, see Fig. 8. It is shown that the increase of the electric field E leads to an enhancement of the magnetization M mainly in the temperature range $T_C \leq T \leq T_N$. Whereas T_N remains unchanged for small couplings K_0, the ferroelectric phase transition temperature T_C is enhanced. The kink is shifted to higher temperatures, near to T_N, and for larger E-values the kink becomes smaller and can disappear completely. The reason is that the electric field shifts the phase transition temperature T_C to higher values and the distance between T_C and T_N shrinks. The saturation magnetization remains likewise unchanged indicating that the magnetic domains do not increase in size. From here we conclude that the domains are

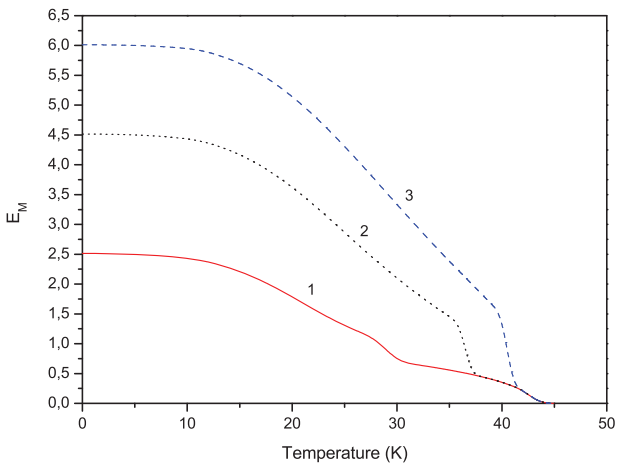

Figure 6 Temperature dependence of the spin-wave-energy $E_M(q = 0)$ for different magnetoelectric couplings: $K_0 = -3\,K$ (1); $-7\,K$ (2); $-10\,K$ (3).

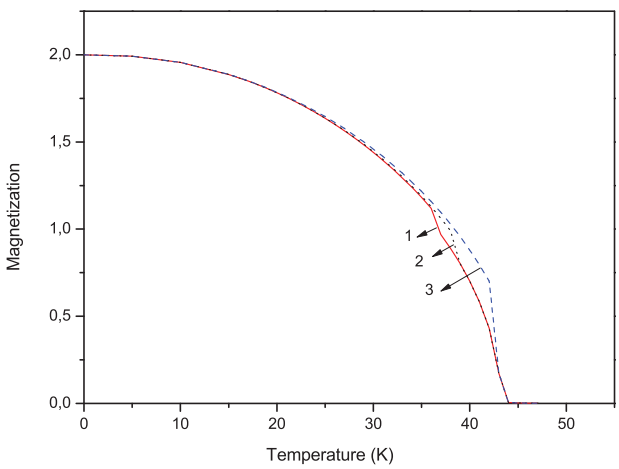

Figure 8 Temperature dependence of the magnetization M for different electric fields E: $E = 0\,K$ (1); $E = 1\,K$ (2); $E = 5\,K$ (3).

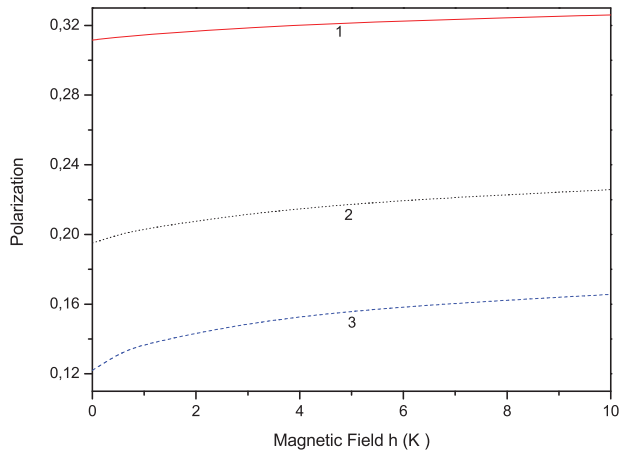

Figure 9 Magnetic field dependence of the polarization P for different temperatures: $T = 24\,\mathrm{K}$ (1); $T = 30\,\mathrm{K}$ (2); $T = 35\,\mathrm{K}$ (3).

just reoriented by the electric field. The calculations suggest that for sufficient high electric field strengths the polarization becomes larger as the magnetization and hence $T_C > T_N$. Then the kink disappears. This theoretical finding should be confirmed by experiments with higher electric fields. Here we present the results for small electric fields. The influence of an external magnetic field h on the polarization P is shown in Fig. 9. The polarization is enhanced with an increasing external magnetic field h. The higher the temperatures the stronger are the changes, compare curve 3 in Fig. 9. Such a behavior is in agreement with the experimental data for $TmMn_2O_5$ [8], $MnWO_4$ [38], and of orthorhombic $YMnO_3$ [39]. The strong MEC is evident in $TbMn_2O_5$ [3], the upward jump in the dielectric constant at T_C transition is pushed to higher temperatures if a magnetic field is applied. The increase of the polarization with the external magnetic field is also in accordance with the results found in Ref. [37]. Using our method we find that the ferroelectric phase transition temperature T_C and the related excitation E_F increase with increasing magnetic field h. Hence the electric phase in the multiferroic compounds RMn_2O_5 can be controlled by an external magnetic field and the dielectric properties turn out to be highly susceptible to such applied fields.

4 Conclusions In spite of the great progress in studying multiferroic materials experimentally there is a current debate on an adequate theoretical description. Here we have studied the influence of the MEC in rare-earth compounds. The presented quantum model is based on the Heisenberg spin model with competing ferromagnetic and antiferromagnetic order. As consequence the magnetic subsystem is frustrated as one feature of the multiferroic material considered. The ferroelectric subsystem is approximately characterized by the Ising model in a transverse field which can be expressed by pseudo-spin operators. The z-component exhibits the two different polarization directions whereas the transverse field simulates the flip-process between the various polarization directions. The system undergoes a magnetic phase transition at temperature T_N. For $T < T_N$ the system offers a finite magnetization which increases with decreasing temperature. At the temperature $T = T_C < T_N$ the system develops due to the magnetoelectric coupling a ferroelectric phase with nonzero polarization. As a result of the symmetry allowed MEC between both order parameters the system becomes multiferroic. Based on this microscopic model we find the excitation spectrum of the multiferroic system at finite temperature. For $T_C < T < T_N$ the system offers conventional Goldstone modes, i.e., gapless spin–wave excitations, the MEC breaks the continuous symmetry of the Heisenberg model and hence the dispersion relation is altered and shows a gap for zero wave vector. The effect is the stronger the higher the MEC is. The appearance of ferroelectricity at T_C is induced by the MEC, where the ferroelectric phase is manifested by a kink in the dispersion relation. As evident by using the Green's function method the excitation spectrum determines the macroscopic quantities as magnetization and polarization. The magnetization is finite in the interval $T_C < T < T_N$ and tends to zero for $T \to T_N$. Owing to the MEC the system offers below T_C simultaneously a finite polarization. Likewise the magnetization is changed in the vicinity of T_C. The effect can be observed for different strengths of the MEC. Finally, the multiferroic system is subjected to external electric and magnetic fields. We find that the polarization increases with growing up magnetic field, i.e., the ferroelectric subsystem can be influenced by a magnetic field. In the same manner the magnetization alters due to an external electric field. Our results suggest that for sufficient high electric fields the phase transition temperature T_C is shifted to higher values and even to $T_C > T_N$. This effect should be observable in experiments. In summary, we have studied a quantum model for multiferroic RMn_2O_5 systems with a magnetoelectric coupling quadratic in the magnetization and linear in the polarization. The microscopic behavior manifested by the excitation spectrum is analyzed and from there we find the macroscopic behavior of the system.

Appendix The Hamiltonian of the ferroelectric subsystem and magnetoelectric coupling reads after rotation

$$
\begin{aligned}
H_f + H_{mf} = & -\Omega \sum_i \left[(1-2\rho_i)\sin\nu + (b_i^\dagger + b_i)\cos\nu)\right] \\
& - \frac{1}{8}\sum_{i,j} J'_{ij} \Big(\left(b_i^\dagger b_j^\dagger + b_i^\dagger b_j + b_i b_j^\dagger + b_i b_j\right)\sin^2\nu \\
& - \left(b_j^\dagger + b_j - 2\rho_i b_j^\dagger - 2\rho_i b_j\right)\sin\nu\cos\nu \\
& - \left(b_i^\dagger + b_i - 2b_i^\dagger\rho_j - b_i\rho_j\right)\sin\nu\cos\nu \\
& + \left(1 - 2\rho_j - 2\rho_i + 4\rho_i\rho_j\right)\cos^2\nu \Big) \\
& + \frac{1}{2}\sum_{ijl} K_{ijl} S_j^z S_l^z \left[(1-2\rho_i)\cos\nu \right. \\
& \left. - (b_i^\dagger + b_i)\sin\nu\right]. \qquad (16)
\end{aligned}
$$

The matrix Green's function obeys

$$\begin{pmatrix} G_q^{(f)11} & G_q^{(f)12} \\ G_q^{(f)21} & G_q^{(f)22} \end{pmatrix} = \begin{pmatrix} 2\langle\sigma_P\rangle & 0 \\ 0 & -2\langle\sigma_P\rangle \end{pmatrix} + \begin{pmatrix} {\varepsilon_q}^{11} & {\varepsilon_q}^{12} \\ {\varepsilon_q}^{21} & {\varepsilon_q}^{22} \end{pmatrix} \begin{pmatrix} G_q^{(f)11} & G_q^{(f)12} \\ G_q^{(f)21} & G_q^{(f)22} \end{pmatrix} \quad (17)$$

with

$$\begin{aligned} {\varepsilon_q}^{11} &= 2\Omega \sin\nu + J_0'\langle\sigma_P\rangle \cos^2\nu - K\cos\nu\langle\sigma_M\rangle^2 \\ &\quad - \frac{1}{2}J_q'\langle\sigma_P\rangle \sin^2\nu, \\ {\varepsilon_q}^{12} &= -\frac{1}{2}J_q'\langle\sigma_P\rangle \sin^2\nu, \\ {\varepsilon_q}^{21} &= -{\varepsilon_q}^{12}, \quad {\varepsilon_q}^{22} = -{\varepsilon_q}^{11}. \end{aligned} \quad (18)$$

The solution for the Green's functions are

$$\begin{aligned} G_q^{(f)11} &= \frac{\langle\sigma_P\rangle\left[E - {\varepsilon_q}^{22}\right]}{\left(E - {\varepsilon_q}^{11}\right)\left(E - {\varepsilon_q}^{22}\right) - \left({\varepsilon_q}^{12}{\varepsilon_q}^{21}\right)}, \\ G_q^{(f)12} &= \frac{-\langle\sigma_P\rangle{\varepsilon_q}^{21}}{\left(E - {\varepsilon_q}^{11}\right)\left(E - {\varepsilon_q}^{22}\right) - \left({\varepsilon_q}^{12}{\varepsilon_q}^{21}\right)}, \\ G_q^{(f)21} &= \frac{\langle\sigma_P\rangle{\varepsilon_q}^{12}}{\left(E - {\varepsilon_q}^{11}\right)\left(E - {\varepsilon_q}^{22}\right) - \left({\varepsilon_q}^{12}{\varepsilon_q}^{21}\right)}, \\ G_q^{(f)22} &= -\frac{\langle\sigma_P\rangle\left[E - {\varepsilon_q}^{11}\right]}{\left(E - {\varepsilon_q}^{11}\right)\left(E - {\varepsilon_q}^{22}\right) - \left({\varepsilon_q}^{12}{\varepsilon_q}^{21}\right)}. \end{aligned} \quad (19)$$

The most relevant function $G^{(f)11}$ can be rewritten in the following general form:

$$G_q^{(f)11} = \langle\sigma_P\rangle\left(\frac{\epsilon_q}{E - E_1} - \frac{\epsilon_q'}{E - E_2}\right) \quad (20)$$

with

$$2E_{1,2}(\boldsymbol{q}) = ({\varepsilon_q}^{11} + {\varepsilon_q}^{22}) \pm \sqrt{({\varepsilon_q}^{11} + {\varepsilon_q}^{22})^2 - 4({\varepsilon_q}^{11}{\varepsilon_q}^{22} - {\varepsilon_q}^{12}{\varepsilon_q}^{21})}. \quad (21)$$

Using the realization presented in Eq. (18) the coefficients in Eq. (11) are given by

$$\begin{aligned} \epsilon_q &= \frac{E_1 - {\varepsilon_q}^{22}}{E_1 - E_2} = \frac{{\varepsilon_q}^{11}}{2E_F(q)} + \frac{1}{2}, \\ \epsilon_q' &= \frac{E_2 - {\varepsilon_q}^{22}}{E_1 - E_2} = \frac{{\varepsilon_q}^{11}}{2E_F(q)} - \frac{1}{2}. \end{aligned} \quad (22)$$

Here we have defined $E_F(\boldsymbol{q}) = \sqrt{({\varepsilon_q}^{11})^2 - ({\varepsilon_q}^{12})^2} \equiv E_1 \equiv -E_2$. The result for $G_q^{(f)11}$ is presented in the text as Eq. (11) where the realizations Eqs. (18) and (22) are used.

Acknowledgements One of us (S.G.B.) acknowledges support by the International Max Planck Research School for Science and Technology of Nanostructures in Halle. J.M.W. is indebted to Max Planck Institute of Microstructure Physics, Halle for financial support.

References

[1] Y. Noda, H. Kimura, M. Fukunaga, S. Kobayashi, I. Kagomiya, and K. Kohn, J. Phys.: Condens. Matter. **20**, 434206 (2008).
[2] T. Kimura, T. Goto, H. Shintani, K. Ishizaka, T. Arima, and Y. Tokura, Nature **426**, 55–58 (2003).
[3] N. Hur, S. Park, P. A. Sharma, J. Ahn, S. Guha, and S. W. Cheong, Nature **429**, 392 (2004).
[4] N. Hur, S. Park, P. A. Sharma, S. Guha, and S. W. Cheong, Phys. Rev. Lett. **93**, 107207 (2004).
[5] S. W. Cheong and M. Mostovoy, Nature Mater. **6**(1), 13–20 (2007).
[6] C. Wang, G. C. Guo, and L. He, Phys. Rev. Lett. **99**, 177202 (2007).
[7] L. C. Chapon, G. R. Blake, M. J. Gutmann, S. Park, N. Hur, P. G. Radaelli, and S. W. Cheong, Phys. Rev. Lett. **93**, 177402 (2004).
[8] M. Fukunaga, Y. Sakamoto, H. Kimura, Y. Noda, N. Abe, K. Taniguchi, T. Arima, S. Wakimoto, M. Takeda, K. Kakurai, and K. Kohn, Phys. Rev. Lett. **103**, 077204 (2009).
[9] Y. S. Oh, B. G. Jeon, S. Y. Haam, S. Park, V. F. Correa, A. H. Lacerda, S. W. Cheong, G. S. Jeon, and K. H. Kim, Phys. Rev. B **83**, 060405 (2011).
[10] J. H. Kim, M. A. van der Vegte, A. Scaramucci, S. Artyukhin, J. H. Chung, S. Park, S. W. Cheong, M. Mostovoy, and S. H. Lee, Phys. Rev. Lett. **107**, 097401 (2011).
[11] J. Koo, C. Song, S. Ji, J. S. Lee, J. Park, T. H. Jang, C. H. Yang, J. H. Park, Y. H. Jeong, K. B. Lee, T. Y. Koo, Y. J. Park, J. Y. Kim, D. Wermeille, A. I. Goldman,G. Srajer, S. Park, and S. W. Cheong, Phys. Rev. Lett. **99**, 197601 (2007).
[12] W. Ratcliff, V. Kiryukhin, M. Kenzelmann, S. H. Lee, R. Erwin, J. Schefer, N. Hur, S. Park, and S. W. Cheong, Phys. Rev. B **72**, 060407 (2005).
[13] T. A. Tyson, M. Deleon, S. Yoong, and S. W. Cheong, Phys. Rev. B **75**, 174413 (2007).
[14] T. Lottermoser, D. Meier, R. V. Pisarev, and M. Fiebig, Phys. Rev. B **80**, 100101 (2009).
[15] T. Kimura, S. Ishihara, H. Shintani, T. Arima, K. T. Takahashi, K. Ishizaka, and Y. Tokura, Phys. Rev. B **68**, 060403 (2003).
[16] J. Hemberger, F. Schrettle, A. Pimenov, P. Lunkenheimer, V. Y. Ivanov, A. A. Mukhin, A. M. Balbashov, and A. Loidl, Phys. Rev. B **75**, 035118 (2007).
[17] C. L. Lu, J. Fan, H. M. Liu, K. Xia, K. F. Wang, P. W. Wang, Q. Y. He, D. P. Yu, and J. M. Liu, Appl. Phys. A **96**, 991 (2009).
[18] L. J. Chang, Y. Su, W. Schweika, T. Brueckel, Y. Y. Chen, D. S. Jang, and R. S. Liu, Physica B **404**, 2517 (2009).
[19] T. Moriya, Phys. Rev. **120**, 91–98 (1960).
[20] A. B. Sushkov, M. Mostovoy, R. Valdes Aguilar, S. W. Cheong, and H. D. Frew, J. Phys.: Condens. Matter **20**, 434210 (2008).
[21] C. Fang and J. Hu, Europhys. Lett. **82**, 57005 (2008).
[22] G. S. Jeon, J. H. Park, J. W. Kim, K. H. Kim, and J. H. Han, Phys. Rev. B **79**, 104437 (2009).

[23] P. G. Radaelli and L. C. Chapon, J. Phys.: Condens. Matter **20**, 434213 (2008).
[24] S. Baidya, P. Sanyal, H. Das, B. Roessli, T. Chatterji, and T. Saha-Dasgupta, Phys. Rev. B **84**, 054444 (2011).
[25] P. Tolédano, W. Schranz, and G. Krexner, Phys. Rev. B **79**, 144103 (2009).
[26] R. Blinc and B. Žekš, Adv. Phys. **21**(93), 693–757 (1972).
[27] R. Pirc and R. Blinc, Phys. Rev. B **70**, 134107 (2004).
[28] J. Wesselinowa, T. Michael, and S. Trimper, in: Handbook of Nanophysics, Vol. 4: Nanoparticles and Quantum Dots, edited by Klaus Sattler (Taylor & Francis, Boca Raton, London, New York, 2010).
[29] K. Taniguchi, N. Abe, T. Takenobu, Y. Iwasa, and T. Arima, Phys. Rev. Lett. **97**, 097203 (2006).
[30] L. C. Chapon, P. G. Radaelli, G. R. Blake, S. Park, and S. W. Cheong, Phys. Rev. Lett. **96**, 097601 (2006).
[31] S. V. Tjablikov, Methods in the Quantum Theory of Magnetism (Plenum Press, New York, 1967).
[32] M. Mostovoy, A. Scaramucci, N. A. Spaldin, and K. T. Delaney, Phys. Rev. Lett. **105**, 087202 (2010).
[33] G. R. Blake, L. C. Chapon, P. G. Radaelli, S. Park, N. Hur, S. W. Cheong, and J. Rodriguez-Carvajal, Phys. Rev. B **71**, 214402 (2005).
[34] W. Nolting, Fundamentals of Many-Body Physics (Springer-Verlag, Berlin, 2009).
[35] J. M. Wesselinowa and I. Georgiev, Phys. Status Solidi B **245**, 1653 (2008).
[36] H. Zheng, J. Wang, S. E. Lofland, S. Ma, L. Mohaddes-Ardabili, T. Zhao, L. Salamanca-Riba, S. R. Shinde, S. B. Ogale, F. Bai, D. Viehland, Y. Jia, D. G. Schlom, M. Wuttig, A. Roytburd, and R. Ramesh, Science **303**, 661 (2004).
[37] N. Leo, D. Meier, R. V. Pisarev, N. Lee, S. W. Cheong, and M. Fiebig, Phys. Rev. B **85**, 094408 (2012).
[38] R. P. Chaudhury, B. Lorenz, Y. Q. Wang, Y. Y. Sun, and C. W. Chu, Phys. Rev. B **77**, 104406 (2008).
[39] I. Fina, L. Fabrega, X. Marti, F. Sanchez, and J. Fontcuberta, Appl. Phys. Lett. **97**, 232905 (2010).

